Steel and Composite Structures, *Vol. 18, No. 6 (2015) 1369-1389*
DOI: http://dx.doi.org/10.12989/scs.2015.18.6.1369

Static behaviour of lying multi-stud connectors in cable-pylon anchorage zone

Zhaofei Lin [1], Yuqing Liu [*1] and Jun He [2]

[1] *Department of Bridge Engineering, Tongji University, Shanghai, China*
[2] *School of Civil Engineering and Architecture, Changsha University of Science and Technology, Hunan, China*

(*Received June 17, 2014, Revised November 14, 2014, Accepted November 25, 2014*)

Abstract. In order to investigate the behaviour of lying multi-stud connectors in cable-pylon anchorage zone, twenty-four push-out tests are carried out with different stud numbers and diameters. The effect of concrete block width and tensile force on shear strength is investigated using the developed and verified finite element model. The results show that the shear strength of the lying multi-stud connectors is reduced in comparison with the lying single-stud connector. The reduction increases with the increasing of the number of studs in the vertical direction. The influence of the stud number on the strength reduction of the lying multi-stud connectors is decreased under combined shear and tension loads compared with under pure shear. Yet, due to multi-stud effect, they still can't be ignored. The concrete block width has a non-negligible effect on the shear strength of the lying multi-stud connectors and therefore should be chosen properly when designing push-out specimens. No obvious difference is observed between the strength reductions of the studs with 22 mm and 25 mm diameters. The shear strengths obtained from the tests are compared with those predicted by AASHTO LRFD and Eurocode 4. Eurocode 4 generally gives conservative predictions of the shear strength, while AASHTO LRFD overestimates the shear strength. In addition, the lying multi-stud connectors with the diameters of 22 m and 25 mm both exhibit adequate ductility according to Eurocode 4. An expression of load-slip curve is proposed for the lying multi-stud connectors and shows good agreement with the test results.

Keywords: cable-pylon anchorage zone; lying multi-stud connectors; push-out tests; strength reduction; load-slip relationship; FEM analysis

1. Introduction

The connection between stay cable and pylon is one of the most critical components in cable-stayed bridges. For cable-stayed bridges with concrete pylons, steel anchor boxes/beams are increasingly used to resist the horizontal component of cable forces. Stud connectors are usually used at the interface between steel flange plate and concrete pylon to transfer the vertical component of cable forces (Su *et al*. 2012, Zheng *et al*. 2014), as shown in Fig. 1. Therefore, the behaviour of stud connectors in this region is of great importance.

Stud connectors are commonly used in steel-concrete composite beams to connect concrete slabs to top flanges of steel beams. In this case, stud connectors are in vertical position when

*Corresponding author, Professor, E-mail: yql@tongji.edu.cn

http://www.techno-press.org/?journal=scs&subpage=8 ISSN: 1229-9367 (Print), 1598-6233 (Online)

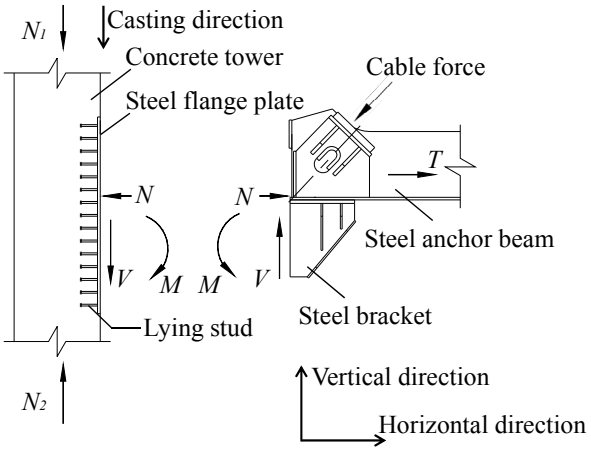

Fig. 1 Mechanical model of lying studs in the cable-tower anchorage area

casting the concrete. Their behaviours have been extensively studied (Viest 1956, Oehlers and Coughlan 1986, Johnson 2000, Badie *et al*. 2002, Lam and EI-Lobody 2005, Xue *et al*. 2012, Hou *et al*. 2012, Abbu *et al*. 2014). However, when the studs are used in the connection between steel anchor box/beam and concrete pylon, they are laid in horizontal direction. According to Kuhlmann and Kürschner (2001), the lying studs show different behaviour in comparison with the vertical studs because of the weaker constraint by the thin concrete slab. Kim and Shim (2009) investigates the shear behaviour of lying studs and find that the nominal strength from the push-out tests is lower than the design values of EC4. In addition, due to the limited area of steel flange plate and the large cable forces, stud connectors are usually arranged vertically and transversally with small spacing. Hence, studs in this rgion can be categorized into multi-stud connectors. Xue *et al*. (2012) study the influence of arrangement and longitudinal spacing of the vertical multi-stud connectors and finds that the shear strength is reduced and the load-slip curve presents different behaviour in comparison with those of the single-stud connector. In ACI 318-08 (2008), when calculating the design strength of stud connectors, a smaller strength reduction factor for shear than for tension is suggested to consider the possibility of a non-uniform distribution of shear in connections with multiple studs.

Moreover, some studs in the anchorage zone are subjected to combined shear and tension loads due to the bending moment acting on the steel flange plate. The shear strength of vertical studs decreases due to the presence of tension force according to McMackin *et al*. (1973), Bode and Roik (1987), Saari *et al*. (2004), Mirza and Uy (2010) and Shen and Chung (2011). Therefore, the behaviour of the stud connectors in cable-pylon anchorage zone may be different with that of the studs in composite beams, which results in a need for research.

In this paper, twenty-four push-out tests are carried out to investigate the shear behaviour of the lying multi-stud connectors in the cable-pylon anchorage zone. The influence of number of studs and stud shank diameter are studied. Based on the experimental results, shear strength and ductility are evaluated and a new expression of load-slip curve is proposed for lying multi-stud connectors. Moreover, a finite element model is developed and verified by the test results. The influence of concrete block width and tension force on the shear strength is investigated using the finite element model.

2. Experimental works

2.1 Test specimens

Twenty-four push-out specimens, divided into eight groups, are prepared and tested. Fig. 2 illustrates the dimensions of the push-out specimens and the arrangement of stud connectors. The parameters chosen are number of studs and stud shank diameter. The number of studs, n, in each steel flange is chosen as 2, 4, 6 and 9. The stud diameters are 22 mm and 25 mm. The height of the studs is 200 mm for all the specimens. The behaviour of the lying single-stud connector is investigated using the specimens with two studs welded on the steel flange in one row. The other specimens with more than two studs are employed to investigate the behaviour of the lying multi-stud connectors. Among the eight groups, SS-22-2, SS-22-4, SS-22-6 and SS-22-9 represent the specimens having 2, 4, 6 and 9 studs with the diameter of 22 mm welded to each steel flange, respectively. Similarly, the other four groups with 25mm studs are denoted as SS-25-2, SS-25-4, SS-25-6 and SS-25-9. Both the vertical and transverse center to center spacing of studs are 150 mm for all the specimens. The studs' size and spacing are selected based on the actual construction details. The diameters of the stirrups and the longitudinal reinforcement are 12 mm and 25 mm, respectively. It should be mentioned that the concrete block width is 600 mm for the specimens with nine studs, and 450 mm for the other specimens. The reason behind it is to keep the same distance from the outer studs to the side edges. Each concrete block is casted in vertical position, as is done for the cable-pylon anchorage in practice. Bond and friction at the steel-concrete interface are avoided and reduced by greasing the flanges.

2.2 Material properties

Three concrete cubic specimens (150 mm × 150 mm × 150 mm) are prepared to determine the concrete compressive strength when casting the push-out specimens. The nominal compressive

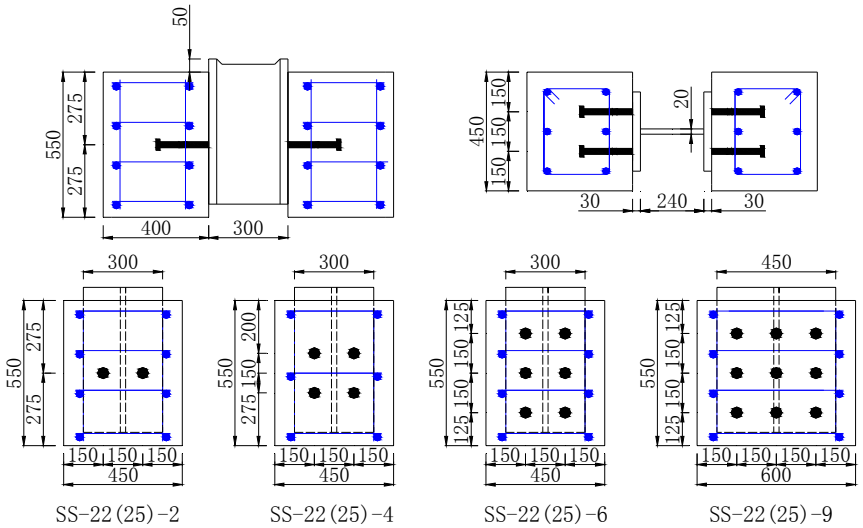

Fig. 2 Test specimens (mm)

Table 1 Material properties of concrete (MPa)

Nominal strength	Compressive strength	Elastic modulus
50	56.3	34545

Table 2 Properties of steel materials (MPa)

Materials	Yield strength		Tensile strength	
	Nominal	Test	Nominal	Test
Headed stud	320	406	400	519
Reinforcement	335	349	—	419
Steel plate	345	437	—	565

strength of concrete is identical to the actual bridge. The cubic specimens are air-cured and tested at 28 days. The material properties of concrete are summarized in Table 1.

Tensile Coupon tests are carried out to determine the material properties of headed studs, structural steel and reinforcement, respectively. The test results are summarized in Table 2. They are provided by the manufactures and also are identical with the actual bridge.

2.3 Loading procedure and measurement

As shown in Fig. 3, push-out specimens are tested in a hydraulic testing machine. In order to apply the load uniformly, a thick steel plate is placed on the top of the steel beam. Fine sands are spread on the surface of the base to avoid uneven loading. Force control is applied with a rate of 5 kN/min till 70% of the expected failure load. Subsequently, displacement control is used until the load dropped to 80% of the maximum load or obvious failure of the specimen is observed. The loading rate for the latter stage is 0.5 mm/min. The slip between the concrete block and steel beam is measured continuously during loading using four 1/1000 LVDTs.

3. Test results and discussion

3.1 Failure modes

The failure mode of all the specimens is governed by stud shearing failure. Cracks are observed at the steel-concrete interface at ultimate load for one specimen with four studs, and a small region of concrete under the stud root is crushed, as presented in Fig. 4. Fig. 4(b) illustrates the observed cracks, where each crack is shown by a red line. Both Type (a) cracks below the stud roots and Type (b) cracks above the stud roots extend to the edges of the concrete block, which are also observed by other researchers (Shim *et al*. 2004, Okada *et al*. 2006, Xue *et al*. 2012, Xu *et al*. 2012).

Type (c) cracks are also observed in the concrete between the studs in the same row, which are also noticed in other researches, as summarized in Table 3. When the stud diameter is 20 mm, Type (c) cracks occur in the specimens whose transverse spacing between studs is 80 mm, whereas such cracks are not found for those with spacing of 100 mm. As the stud diameter increases to

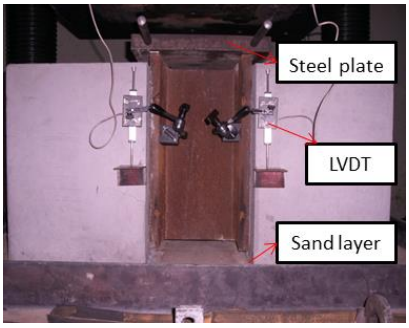

Fig. 3 Test set-up

(a) SS-22-2-1

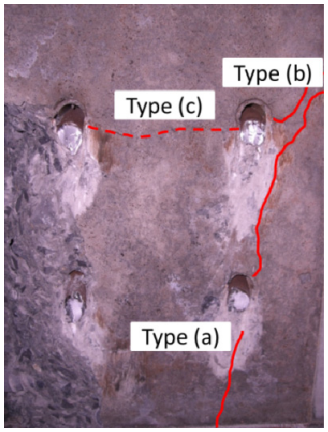

(b) SS-22-4-1

Fig. 4 Failure mode

Table 3 Transverse cracks at the interface (mm)

Researchers	Transverse spacing	Stud diameter	Cracks
Xu *et al*. (2012)	50	13	appear
Okada *et al*. (2006)	80	22	appear
Xue *et al*. (2012)	100	22	not appear
Authors	150	22/25	not appear
Shim *et al*. (2004)	100	27/30	appear

27/30 mm, Type (c) cracks start to appear for the specimens with spacing of 100 mm. This indicates that with the increasing of the stud diameter, Type (c) cracks may occur in a larger transverse spacing. Therefore, if large diameter studs are adopted in design, an appropriate spacing of the studs should be chosen to avoid the Type (c) cracks.

3.2 Shear strength

Shear strength, V_u, is defined as the maximum load per stud during loading process. Table 4 summarizes the test results. For both the 22 mm and 25 mm lying multi-stud connectors, the shear strength is reduced in comparison with that of the lying single-stud connector, as shown in Fig. 5. The reduction percentage increases with the increasing of the number of studs in the vertical direction but decreases when the number of studs increases from two to three in transverse direction. For the specimens with 4, 6, 9 studs on each steel flange, the average reductions are 2.8%, 10.7% and 3.2%, respectively, for 22 mm studs and 3.5%, 9.3% and 2.6%, respectively, for 25 mm studs. The maximum reductions are 13.2% and 9.9% for 22 mm and 25 mm studs, respectively. No obvious difference is found between the reductions of 22 mm and 25 mm studs. The shear strength reductions of the specimens with nine studs are smaller than those of the specimens with six studs, which is due to the difference of concrete block width as verified by the following parametric studies.

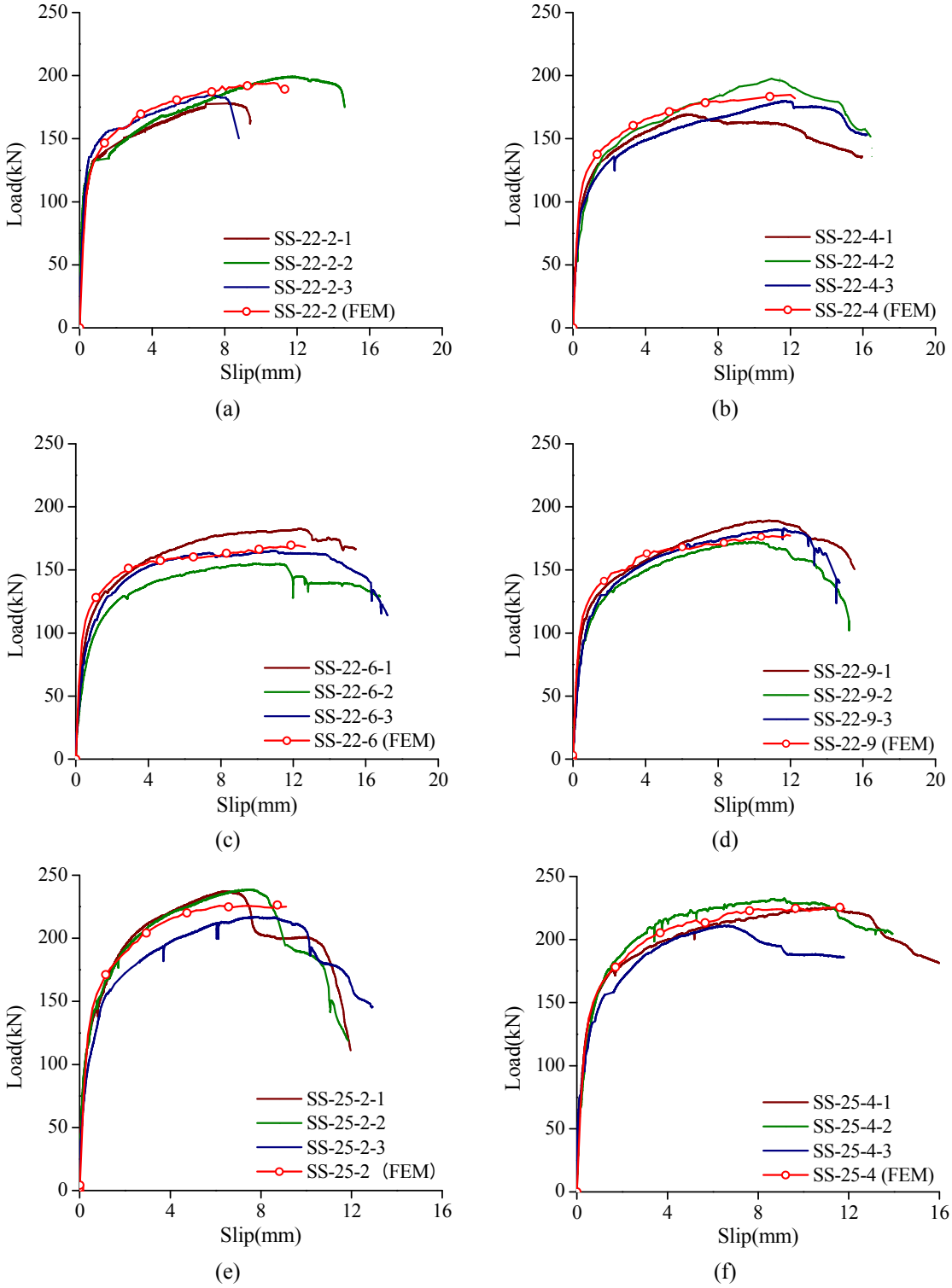

Fig. 5 Load-slip curves

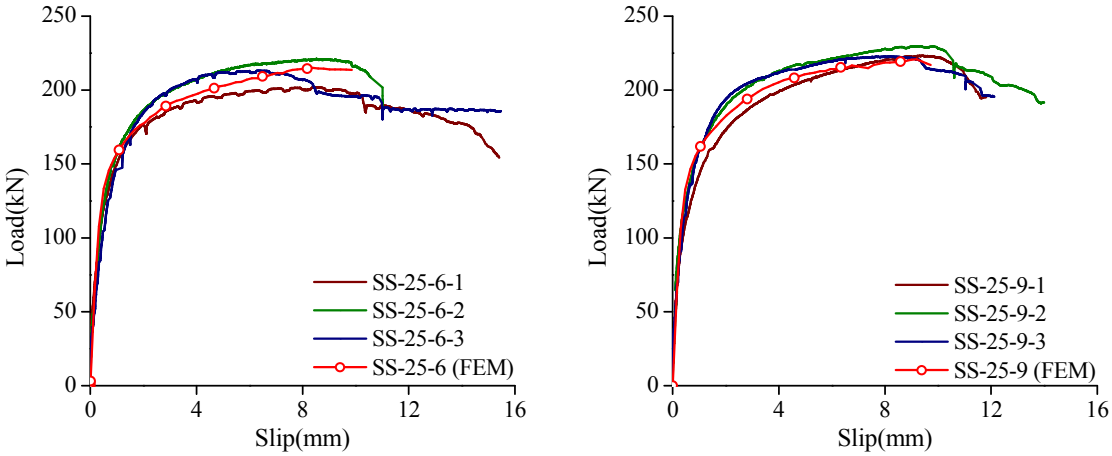

Fig. 5 Continued

The applicability of some existing shear strength equations to the lying multi-stud connectors is evaluated herein. The equation proposed by Kim and Shim (2009) for computing the shear strength of lying studs is adopted. The shear strength equations specified in EC4 (2004) and AASHTO LRFD (2007) are also evaluated. The three equations are of the following form

$$V_{u,Kim} = 0.725 A_{sc} f_u \tag{1}$$

$$V_{u,EC4} = \min\left(0.29\alpha d^2 \sqrt{E_{cm} f_{ck}},\ 0.8\pi d^2 f_u / 4\right) \tag{2}$$

$$V_{u,AASHTO\ LRFD} = 0.5 A_{sc} \sqrt{E_{cm} f_{ck}} \le A_{sc} f_u \tag{3}$$

where d is the stud shank diameter (mm), A_{sc} is the cross area of the stud shank (mm^2), f_{ck} is the concrete compressive strength (MPa), E_{cm} is the Young's modulus of concrete (MPa), f_u is the ultimate strength of the stud material (MPa). In our evaluation, for the purpose of comparison, the partial factor and the resistance factor are set to be 1.0. The comparison of the shear strength obtained from the tests and those derived from Eqs. (1)-(3) are made and illustrated in Fig. 6. It can be concluded that those equations are not able to reflect the influence of the number of studs.

The mean values of the ratios of $V_{u,Kim} / V_{u,test}$ $V_{u,EC4} / V_{u,test}$ and $V_{u,AASHTO\ LRFD} / V_{u,test}$ are 0.76, 0.84 and 1.06 with the corresponding coefficients of variations of 0.047, 0.053 and 0.052, respectively, for the single-stud connector. The mean values of the ratios are 0.81 0.90 and 1.12 with the corresponding coefficients of variations of 0.070, 0.073 and 0.071, respectively, for the multi-stud connectors. Eq. (1) gives the most conservative predictions. EC4 generally yield less conservative values and predict the shear strength of the multi-stud connectors with acceptable accuracy. AASHTO LRFD overestimates the shear strength but provide reasonable predictions of the lying single-stud connector. It should be mentioned that the studs are aligned in three rows with one stud per row in Kim's research, and the standard arrangement specified by EC4 has four studs on each flange with two studs per row.

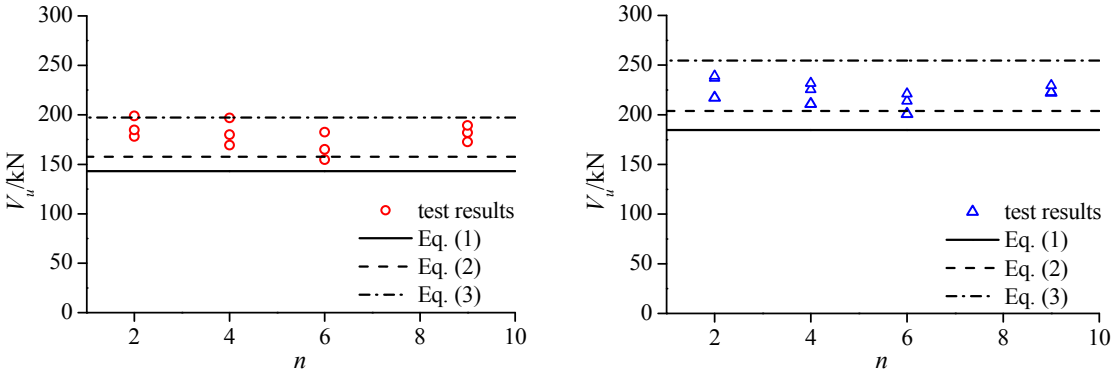

(a) 22 mm studs (b) 25 mm studs

Fig. 6 Comparison of shear strength obtained from the tests and calculated by different strength equations

3.3 Peak/ultimate slip

Peak slip, s_p, is defined as the slip at the maximum load, and ultimate slip, s_u, is the slip at the 90% of the maximum load on the post-peak descending branch. According to EC4, the characteristic ultimate slip, δ_{uk}, can be taken as the minimum tested ultimate slip reduced by 10% and the stud connector can be taken as ductile if the characteristic ultimate slip is at least 6 mm.

The test results are presented in Table 4. It can be seen that the average values of the peak slip, the ultimate slip and the characteristic slip of the multi-stud connectors are larger than those of the single-stud connector for both 22 mm and 25 mm studs. The average characteristic ultimate slip of the multi-stud connectors with 25 mm diameter is about 21% less than that of the multi-stud connectors with 22 mm studs; nevertheless, they are all larger than 6 mm. Therefore, the slip capacity of the multi-stud connectors satisfies the requirement of EC4.

3.4 Load-slip relationship

The load-slip curves are presented in Fig. 5. Previous researchers (Oehlers and Coughlan 1986 Shim *et al*. 2004) find that the load-slip relationship of vertical studs is nearly linear up to 50% of the maximum load, which is consistent with the curves of the lying studs in this study. Besides, the shear force in studs usually is usually not greater than half of the maximum load under serviceability limit states. Hence the shear stiffness, k_e, is defined as the secant modulus at the point where the applied load is half of the maximum load for the lying studs in this study. Table 4 shows the shear stiffness of each test specimen.

Several equations have been proposed for computing the load-slip behaviour of vertical studs. Eq. (4) is proposed by Ollgard *et al*. (1971) and has been widely referred and adopted. Xue *et al*. (2012) proposes an empirical expression for vertical multi-stud connectors, as shown in Eq. (5). However, to the best of our knowledge, no equation is available in the literature for lying multi-stud connectors. Comparisons between Eq. (4), Eq. (5) and the tested curves are made, and the comparison results are shown in Fig. 7.

$$\frac{V}{V_u} = (1 - e^{-0.71S})^{0.4} \tag{4}$$

Table 4 Test results

Groups	Test No.	V_u (kN)				Eq. (1) /Test	Eq. (2) /Test	Eq. (3) /Test	k_e (kN/mm)	s_p (mm)	s_u (mm)	δ_{uk} (mm)
		Test	Eq.(1)	Eq.(2)	Eq.(3)							
SS-22-2	1	178.2				0.80	0.89	1.11	332.1	7.01	9.41	7.70
	2	198.8	143.0	157.8	197.2	0.72	0.79	0.99	523.2	11.35	14.61	
	3	184.6				0.77	0.85	1.07	383.8	7.36	8.55	
	mean	**187.2**	**143.0**	**157.8**	**197.2**	**0.77**	**0.84**	**1.06**	**413.0**	**8.57**	**10.86**	
SS-22-4	1	169.4				0.84	0.93	1.16	268.3	6.27	12.91	11.62
	2	196.9	143.0	157.8	197.2	0.73	0.80	1.00	130.3	10.87	14.73	
	3	179.9				0.79	0.88	1.10	207.6	11.61	15.10	
	mean	**182.1**	**143.0**	**157.8**	**197.2**	**0.79**	**0.87**	**1.09**	**202.1**	**9.58**	**14.25**	
SS-22-6	1	182.4				0.78	0.87	1.08	180.2	12.41	15.30	11.57
	2	154.7	143.0	157.8	197.2	0.92	1.02	1.27	134.2	10.97	12.85	
	3	165.1				0.87	0.96	1.19	177.7	10.82	15.41	
	mean	**167.4**	**143.0**	**157.8**	**197.2**	**0.86**	**0.95**	**1.18**	**164.0**	**11.40**	**14.52**	
SS-22-9	1	189.2				0.76	0.83	1.04	240.7	10.78	14.35	11.99
	2	172.5	143.0	157.8	197.2	0.83	0.91	1.14	172.5	9.43	13.32	
	3	181.9				0.79	0.87	1.08	167.4	10.97	13.73	
	mean	**181.2**	**143.0**	**157.8**	**197.2**	**0.79**	**0.87**	**1.09**	**193.5**	**10.39**	**13.80**	
SS-25-2	1	236.9				0.80	0.89	1.11	288.9	6.34	7.58	6.82
	2	239.9	184.6	203.7	254.6	0.72	0.79	0.99	291.5	7.34	8.75	
	3	217.0				0.77	0.85	1.07	216.7	7.51	10.16	
	mean	**231.3**	**184.6**	**203.7**	**254.6**	**0.77**	**0.84**	**1.06**	**265.7**	**7.06**	**8.83**	
SS-25-4	1	225.4				0.84	0.93	1.16	352.2	10.46	13.61	8.31
	2	231.6	184.6	203.7	254.6	0.73	0.80	1.00	264.6	8.64	12.78	
	3	210.7				0.79	0.88	1.10	280.2	6.34	9.23	
	mean	**222.6**	**184.6**	**203.7**	**254.6**	**0.79**	**0.87**	**1.09**	**299.0**	**8.48**	**11.87**	
SS-25-6	1	200.7				0.78	0.87	1.08	312.5	7.02	13.28	9.86
	2	221.1	184.6	203.7	254.6	0.92	1.02	1.27	276.3	8.52	10.95	
	3	213.7				0.87	0.96	1.19	212.8	6.30	10.98	
	mean	**211.8**	**184.6**	**203.7**	**254.6**	**0.86**	**0.95**	**1.18**	**267.2**	**7.28**	**11.74**	
SS-25-9	1	222.7				0.76	0.83	1.04	224.8	9.25	11.41	10.27
	2	229.5	184.6	203.7	254.6	0.83	0.91	1.14	327.9	8.99	12.13	
	3	222.1				0.79	0.87	1.08	270.9	7.76	11.61	
	mean	**224.8**	**184.6**	**203.7**	**254.6**	**0.79**	**0.87**	**1.09**	**274.5**	**8.67**	**11.72**	

$$\frac{V}{V_u} = (1 - e^{-0.7S})^{1/3} \tag{5}$$

$$\frac{V}{V_u} = (1 - e^{-0.5S})^{0.5} \tag{6}$$

It can be seen that the ascending branches of the lying multi-stud connectors are much slower than those of the vertical studs. Therefore, based on the analysis of the tests, a new equation is proposed, as shown by Eq. (6). Table 5 presents the comparison of the slips predicted by Eqs. (4)-(6) and those obtained from the tests at $0.3V_u$, $0.5V_u$, $0.7V_u$ and $0.9V_u$. It can be noted that Eq. (6) gives the most accurate predictions.

Table 5 Comparison of expressions of load-slip curves

Groups	Test No.	*s* (mm)			
		0.3 V_u	0.5 V_u	0.7 V_u	0.9 V_u
SS-22-4	1	0.11	0.32	0.97	3.72
	2	023	0.76	1.71	6.43
	3	0.19	0.43	1.61	6.62
SS-22-6	1	0.21	0.51	1.35	4.94
	2	0.24	0.58	1.31	4.15
	3	0.21	0.46	1.27	3.52
SS-22-9	1	0.17	0.39	1.46	5.83
	2	0.20	0.50	1.39	4.89
	3	0.24	0.54	1.38	5.34
SS-25-4	1	0.12	0.32	0.94	4.35
	2	0.14	0.44	1.01	3.25
	3	0.09	0.38	0.97	3.12
SS-25-6	1	0.13	0.32	0.79	2.5
	2	0.21	0.40	0.93	3.00
	3	0.14	0.50	1.09	2.37
SS-25-9	1	0.14	0.50	1.29	4.14
	2	0.14	0.35	1.05	3.29
	3	0.20	0.41	0.91	2.35
	mean	**0.17**	**0.45**	**1.16**	**3.93**
	CV	**0.29**	**0.24**	**0.24**	**0.38**
Eq. (4)/test	**mean**	**0.41**	**0.62**	**0.64**	**0.52**
Eq. (5)/test	**mean**	**0.29**	**0.42**	**0.52**	**0.47**
Eq. (6)/test	**mean**	**1.10**	**1.21**	**1.16**	**0.85**

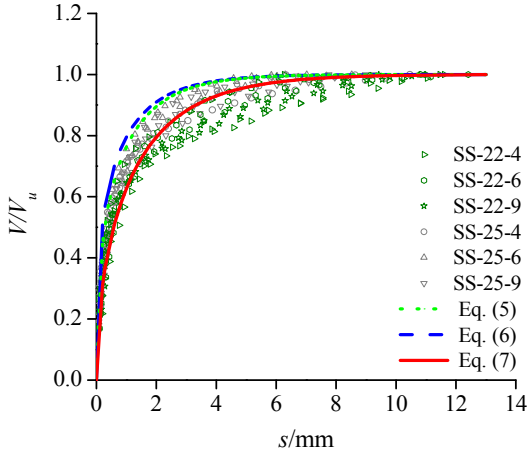

Fig. 7 Comparison of expressions of load-slip curves

4. Finite element model

4.1 General

In this study, the finite element program ABAQUS (2010) is used to simulate the push-out tests and the dynamic explicit analysis method is employed. In the finite element model, the main components of the push-out specimen, including the concrete blocks, the steel beams, the reinforcements and the stud connectors are simulated. Material nonlinearity and the interaction between different components are properly considered. Different mesh sizes, element types and interactions are also studied to ensure a reliable and efficiency model.

4.2 Element type and mesh

Element type greatly influences the accuracy and efficiency of the modeling. Both C3D20R and C3D8R are used to simulate the concrete block and headed stud. C3D20R is a three-dimensional quadratic brick element with a quadratic approximation of displacements, reduced integration of twenty nodes and three translational degrees of freedom. C3D8R is a three-dimensional eight-node element with a linear approximation of displacements. C3D20R can capture the stress concentration more effectively and is better for modeling geometric features (Mirza and Uy 2010). However, the investigations show that C3D8R is able to give the same accurate predictions as C3D20R if the mesh size is fine enough and is less time-consuming. Therefore, C3D8R is chosen to simulate the concrete block, headed stud and steel beam. Reinforcement is modeled by truss element T3D2.

The mesh in the failure region is critical to derive accurate predictions. The effects of mesh sizes are studied. The results show that the mesh with 16 elements in circumference of the hole almost predicts the same load-slip relation compared with those with finer meshes. The mesh size along stud shank is 0.2 times of its diameter, which gives more accurate predictions of the failure mode and load-slip curve. Coarse mesh is applied in other regions in order to save the computation time. In addition, 1/4 model, as shown in Fig. 8, is adopted because of the symmetry of the specimens in order to improve the efficiency of analysis.

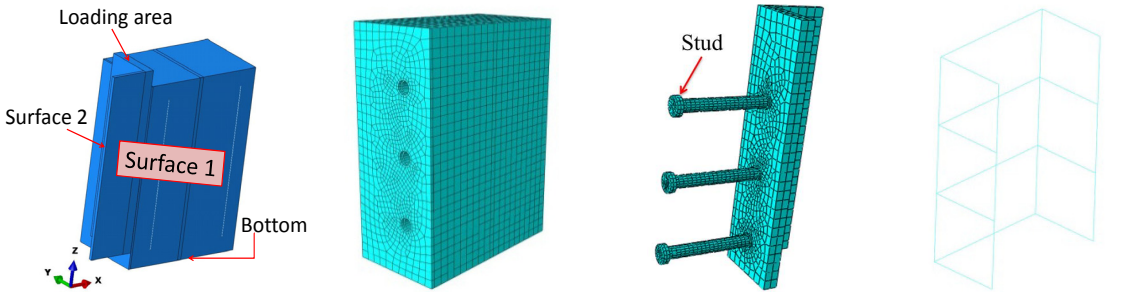

(a) Model (b) Concrete block (c) Steel components (d) Reinforcements

Fig. 8 The finite element model

4.3 Interaction

Two types of interaction, contact interaction and tie constraint, are employed to simulate the interface behaviour between studs and concrete blocks in previous researches (Mirza and Uy 2010, Nguyen and Kim 2009, Qureshi *et al*. 2011). The investigations show that tie constraint overestimates both shear stiffness and shear strength. Thus, contact interaction is employed at the interface. The hard contact and penalty frictional formulation are used to simulate the normal and tangential behaviour of the interface between the stud and concrete block, respectively. The coefficient of friction is taken as 0.4 according to the experimental results of Cook and Klingner (1989). The interaction between the steel beam and the concrete block is modeled by hard contact in the normal direction and frictionless in the tangential direction because of the greased flange. The embedded constrain is applied to the reinforcing elements and concrete elements. Perfect bond between reinforcement and surrounding concrete is assumed without considering the slip and debond of reinforcement.

4.4 Loading and boundary conditions

Symmetric boundary condition is applied to surface 1 and surface 2 at the symmetric planes of the specimen, as shown in Fig. 8(a). The surface 1 and surface 2 are taken as symmetric in Y direction and X direction, respectively. The translational movement U_z at the bottom surface of the concrete slab is restrained. The vertical displacement as shear loading is applied at the top of the steel beam.

4.5 Material modeling

4.5.1 Concrete

The stress-strain curve proposed by Carreira and Chu (1985), as shown in Fig. 9 and Eq. (7), is adopted to simulate the concrete compressive behaviour since it has been employed and verified by other researchers (Mirza and Uy 2010). The stress-strain relationship is assumed to be linear up to 40% of the compressive strength.

$$\sigma_c = \frac{f_c \gamma (\varepsilon_c / \varepsilon_c')}{\gamma - 1 + (\varepsilon_c / \varepsilon_c')^{\gamma}} \tag{7}$$

where σ_c = compressive stress, f_c = the compressive strength of concrete, ε_c = compressive strain, ε'_c = strain corresponding to the compressive strength; and $\gamma = (f_c/32.4)^3 + 1.55$, $\varepsilon'_c = 0.002$.

The tensile stress, σ_t, on the other hand, is assumed to increase linearly until the ultimate stress, f_t, and the stress-displacement relationship proposed by Cornelissen *et al*. (1986) is adopted to simulate the post-crack part, as shown in Fig. 10 and Eqs. (8)-(9). G_f is the energy required to open a unit area of crack using brittle fracture concepts, which is calculated using Eq. (10) (FIB 55 2010). The reason why stress-displacement relationship is used to simulate the post-failure behaviour is that the stress-strain relationship would introduce unreasonable mesh sensitivity into results if there aren't enough reinforcements in significant regions of the model (ABAQUS 2010).

$$\frac{\sigma_t}{f_t} = f(\omega) - \frac{\omega}{\omega_c} f(\omega_c) \tag{8}$$

$$f(\omega) = \left[1 + \left(\frac{c_1\omega}{\omega_c}\right)^3\right] e^{\left(-\frac{c_2\omega}{\omega_c}\right)} \tag{9}$$

$$G_f = 73 f_c^{0.18} \tag{10}$$

where ω = cracking displacement, ω_c = failure cracking displacement; and $\omega_c = 5.14 G_f/f_t$, $c_1 = 3.0$, $c_2 = 6.93$ for normal density concrete.

4.5.2 Steel materials

The stress-strain relationship of structural steel, reinforcement steel and stud are plotted in Figs. 11-13, respectively. The tri-linear model with strain hardening is used to simulate the behaviour of stud material. The stress-strain relationship for structural steel and reinforcement steel used by Loh *et al*. (2004) are adopted herein. f_{ys}, f_{us} and ε_{ys} are the yield stress, the ultimate strength and the yield strain of structural steel, respectively. f_{yr}, f_{ur} and ε_{yr} are the yield stress, the ultimate strength and the yield strain of reinforcement, respectively. f_{yst}, f_{ust} and ε_{yst} are the yield stress, the ultimate

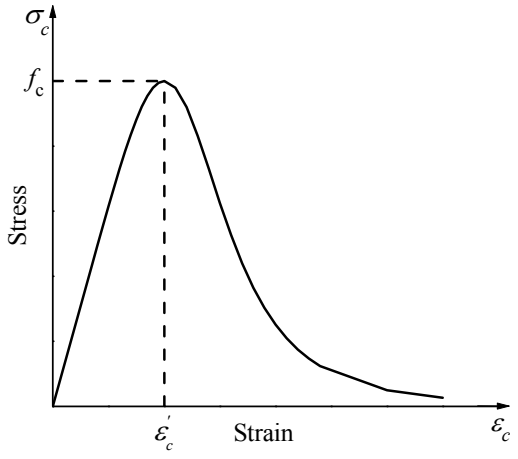

Fig. 9 Constitutive law for concrete under compression

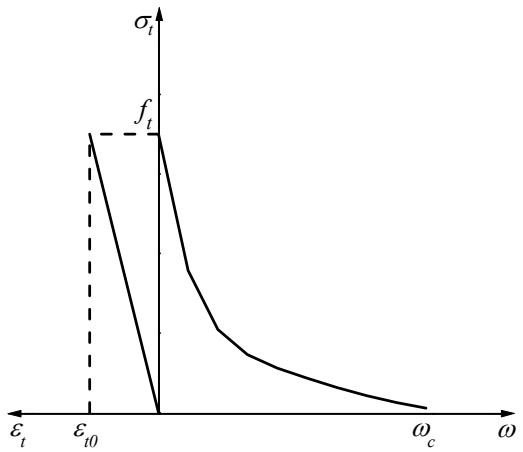

Fig. 10 Constitutive law for concrete under tension

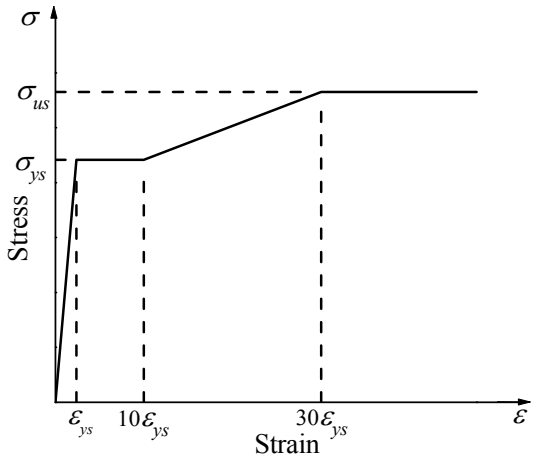

Fig. 11 Constitutive law for structural steel

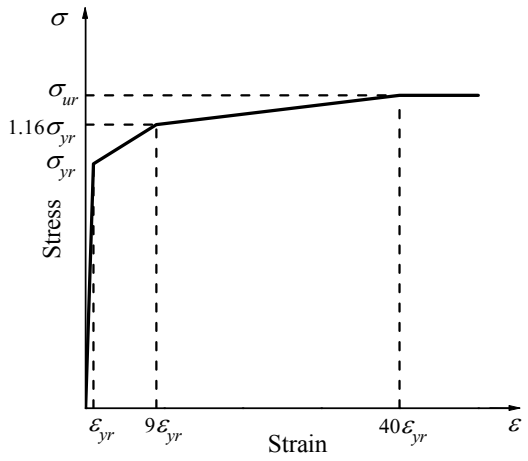

Fig. 12 Constitutive law for reinforcement steel

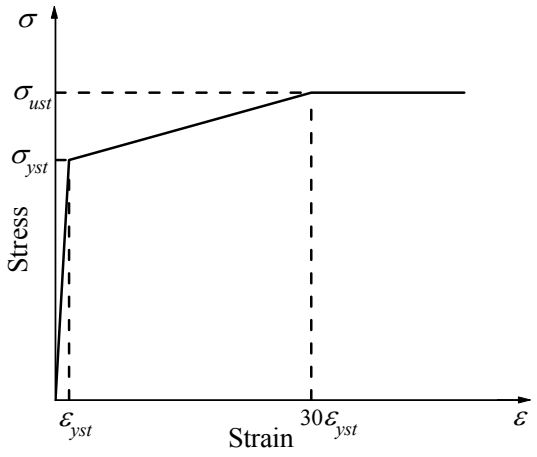

Fig. 13 Constitutive law for studs

strength and the yield strain of stud matrial, respectively.

4.6 Verification of finite element model

For comparison and verification purpose, mean values of the material properties obtained from the experiments are adopted in the finite element analysis. The failure mode observed from the finite element analysis is governed by the stud shearing failure. The stress of the concrete around the stud root reaches the cracking stress after the studs reach the ultimate strength for the specimens with multiple studs, which are similar to the test results. Fig. 5 shows the comparison of the load-slip curves derived from the finite element analysis and tests. A good agreement has been achieved.

The shear strength, shear stiffness and peak slip obtained from the finite element analysis are summarized in Table 6 and are compared with the mean values of the test results. The maximum

Table 6 Comparison of the results obtained from finite element analysis and the tests

Specimen	$V_{u,\mathrm{FEM}}$ (kN)	$k_{e,\mathrm{FEM}}$ (kN/mm)	$s_{p,\mathrm{FEM}}$ (mm)	$V_{u,\mathrm{FEM}} / V_{u,\,\mathrm{test},\,avg.}$	$k_{e,\mathrm{FEM}} / k_{e,\,\mathrm{test},\,avg.}$	$s_{p,\mathrm{FEM}} / s_{p,\,\mathrm{test},\,avg.}$
SS-22-2	194.3	294.4	9.64	1.04	0.71	1.12
SS-22-4	184.8	229.1	11.03	1.01	1.13	1.15
SS-22-6	169.5	219.6	12.40	1.01	1.34	1.09
SS-22-9	177.8	275.0	10.99	0.98	1.42	1.06
SS-25-2	230.5	345.1	7.52	1.00	1.30	1.07
SS-25-4	224.5	341.3	7.98	1.01	1.14	0.94
SS-25-6	214.9	319.8	7.95	1.01	1.20	1.09
SS-25-9	221.6	343.8	9.13	0.99	1.25	1.05
mean				**1.01**	**1.19**	**1.07**
CV				**0.021**	**0.182**	**0.065**

differences between the numerical results and the test results are 4%, 42% and 15%, respectively. The mean values of $V_{u,\mathrm{FEM}}/V_{u,\,\mathrm{test},\,avg}$, $k_{e,\mathrm{FEM}}/k_{e,\,\mathrm{test},\,avg}$ and $s_{p,\mathrm{FEM}}/s_{p,\,\mathrm{test},\,avg.}$ ratios are 1.01, 1.19 and 1.07, respectively, with the corresponding coefficients of variations of 0.021, 0.182 and 0.065, respectively. Therefore, the proposed finite element model can reasonably predict the shear behaviour of both the lying single-stud connector and multi-stud connectors and thus is reliable for the following parametric study.

5. Parametric study

There are two purposes to conduct the parametric study. One is to clarify if the smaller strength reductions of the test specimens with nine studs result from the different widths of the concrete blocks and the steel flanges. The other one is to investigate the influence of tension force on the shear strength of the lying multi-stud connectors since some studs in the anchorage zone are subjected to combined shear and tension loads.

In the parametric study, nominal values of the material properties are used in order to compare the shear strength obtained from the parametric analysis with the nominal values computed by the codes. The constitutive models of materials, the boundary conditions and the interaction are set the same as the verified model.

5.1 Influence of the width of concrete blocks

Initially, the specimen with six 22 mm studs is simulated to find whether the influence of the widths of the concrete blocks, b_c, or the steel flanges, b_s, can be ignored. According to the simulated results, the shear strength increased about 5.8% when concrete block width increases from 450 mm to 600 mm, whereas it almost remain constant with the increasing of steel flange width. Therefore, the influence of the concrete slab width can't be ignored.

The parametric studies on eleven specimens are carried out in order to investigate the influence of concrete block width on the strength reduction of multi-stud connectors, as shown in Table 7. The widths of the concrete blocks are chosen as 450, 600 and 900 mm. The width of steel flange is

Table 7 Parametric study under shear loading

Specimen	n	b_c (mm)	$V_{u,\mathrm{FEM}}$ (kN)	$V_{u,\mathrm{FEM}}/V_{u,EC4}$	$V_{u,\mathrm{FEM}}/V_{u,AASHTO}$
A-1	2	450	146.2	1.20	0.96
A-2	4	450	139.3	1.15	0.92
A-3	6	450	132.8	1.09	0.87
B-1	2	600	147.0	1.21	0.97
B-2	4	600	141.5	1.16	0.93
B-3	6	600	141.0	1.16	0.93
B-4	9	600	136.7	1.12	0.90
C-1	2	900	146.1	1.20	0.96
C-2	4	900	140.3	1.15	0.92
C-3	6	900	139.5	1.15	0.92
C-4	9	900	135.8	1.12	0.89

450 mm. The dominant failure mode of the specimens is stud shearing fracture. The reductions of shear strength with respect to the widths of the concrete blocks are illustrated in Fig. 14.

For the 450 mm wide concrete block, the reduction increases with the increasing of the number of studs. The maximum reduction is 9.2% for the specimen with six studs. As for the 600 mm wide concrete block, the reductions also increased with the number of studs. The maximum reduction is 7.0% for the specimen with nine studs. In contrast, the reductions are decreased for the specimens with four and six studs compared to those of the specimens with 450 mm wide concrete blocks. As for the 900 mm concrete block, the reductions are almost identical to those of the 600 mm width concrete block. It also can be noticed that the influence of the concrete block width increases with the increasing of the number of studs when the width is not greater than 600 mm. When exceeding 600 mm, the width has little influence on the strength reduction regardless of the number of studs. Given that the concrete pylon is usually much wider than the steel flange plate, the influence of the concrete block width can be ignored.

Therefore, it can be concluded that the smaller strength reduction of the test specimens with nine studs than the test specimens with six studs is due to the difference of the widths of the concrete blocks. Given that the concrete pylon is usually much wider than the steel flange plate, the width of the concrete block is chosen as 600 mm when investigating the influence of tension force.

5.2 Influence of tension force

In the finite element analysis, tension force is initially applied to the studs by exerting uniform distributed axial force on the back surface of the concrete block and kept constant in the subsequent shear loading. Given that the shear force is dominant in the anchorage zone, the applied tension forces per stud, T, are chosen as $0.1T_u$, $0.2T_u$, $0.3T_u$, $0.4T_u$ and $0.5T_u$, where T_u is the nominal tension strength per stud calculated by equations in ACI 318-08 assuming ductile failure of studs. Assuming ductile failure is reasonable since the failure mode of all the specimens under combined loads is stud fracture according to the finite element results.

The influence of tension force on strength reduction of multi-stud connectors is illustrated in

Fig. 15. The strength reduction increases slower with the increasing of number of studs under combined shear and tension than under shear for the specimens with multiple studs, which indicates that the influence of the number of studs on the strength reduction of the multi-stud connectors becomes less due to the presence of tension force. The shear strengths of the specimens with two studs reduces about 2.9%, 5.9%, 8.4%, 12.5% and 21.3% under $0.1T_u$, $0.2T_u$, $0.3T_u$, $0.4T_u$ and $0.5T_u$, while those of the specimen with nine studs reduces by about 10.5%, 15.2%, 21.7%, 27.7% and 34.6%. Therefore, the influence of the number of studs still cannot be ignored under combined loads.

McMackin *et al*. (1973) and, Bode and Roik (1987) suggest Eqs. (11)-(12), respectively, to determine the interaction strength of studs under combined shear and tension loads. Their applicability to the lying single-stud connector and multi-stud connectors is assessed herein. V_u is computed by Eqs. (2) and (3), and V_{cu} is the maximum shear load under combined loading. The comparison results are summarized in Table 8. When V_u is calculated by Eq. (2), Eqs. (11)-(12) give conservative values of the interaction strengths for both the single-stud connector and the multi-stud connectors. However, when V_u is calculated by Eq. (3), Eqs. (11)-(12) generally overestimates the interaction strengths.

$$\left(\frac{V}{V_u}\right)^{\frac{5}{3}}+\left(\frac{T}{T_u}\right)^{\frac{5}{3}}\le 1 \tag{11}$$

$$\begin{aligned}&\text{If}\quad V\le 0.2V_u \quad \text{or}\quad T\le 0.2T_u, \quad \text{interaction effect can be ignored;}\\ &\text{If}\quad V\ge 0.2V_u \quad \text{and}\quad T\ge 0.2T_u, \quad \text{then}\quad \frac{V}{V_u}+\frac{T}{T_u}\le 1.2\end{aligned} \tag{12}$$

Eq. (13) is proposed by Pallarés and Hajjar (2010) to assess the accuracy of interaction equations. When Eq. (2) is adopted, the mean values of $R_{Eq.(11)}$ and $R_{Eq.(12)}$ are 1.18 and 1.21, with the corresponding coefficients of variations of 0.020 and 0.040, respectively, for the lying single-

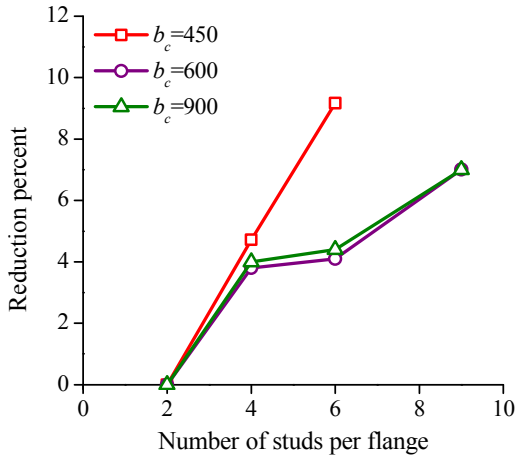

Fig. 14 Influence of widths of concrete blocks on strength reductions

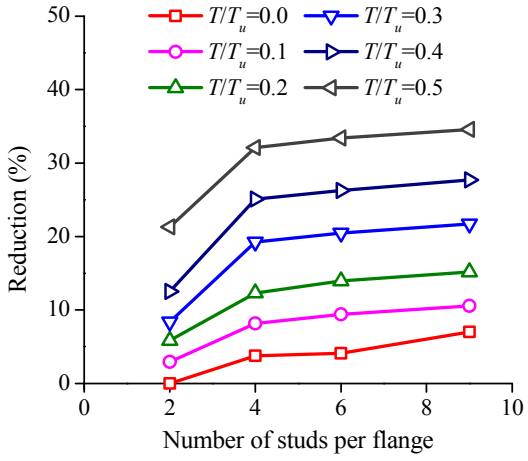

Fig. 15 Influence of tension forces on strength reductions

stud connector and are 1.07 and 1.09, with the corresponding coefficients of variations of 0.049 and 0.035, respectively, for the lying multi-stud connectors. When Eq. (3) is adopted, the mean values of $R_{Eq.(11)}$ and $R_{Eq.(12)}$ are 0.96 and 0.99, with the corresponding coefficients of variations of 0.014 and 0.058, respectively, for the lying single-stud connector and are 0.88 and 0.89, with the corresponding coefficients of variations of 0.028 and 0.043, respectively, for the lying multiple-studs.

$$R = \sqrt{\frac{\left(\frac{T_{cu}}{T_u}\right)^2_{FEM} + \left(\frac{V_{cu}}{V_u}\right)^2_{FEM}}{\left(\frac{T_{cu}}{T_u}\right)^2_{predicted} + \left(\frac{V_{cu}}{V_u}\right)^2_{predicted}}} \tag{13}$$

According to the assessment results, it can be concluded that Eq. (2) is more accurate for calculating the interaction strength of the lying multi-stud connectors, while Eq. (3) is more accurate for computing the interaction strength of the lying single-stud connector. Both the elliptic and tri-linear equations give reasonable predicted values of the interaction strength of lying multi-stud connectors.

Table 8 Parametric study under combined shear and tension loading

Specimen	T/T_u	n	$V_{cu,FEM}$ (kN)	$V_{cu,FEM}/V_{u,EC4}$	$V_{cu,FEM}/V_{u,AASHTO\ LRFD}$	$(V_{cu}/V_u)_{Eq.(11)}$	$(V_{cu}/V_u)_{Eq.(12)}$
D-2	0.1	2	142.7	1.17	0.94	0.99	1.00
D-4		4	135.0	1.11	0.89		
D-6		6	133.2	1.10	0.88		
D-9		9	131.5	1.08	0.86		
E-2	0.2	2	138.4	1.14	0.91	0.96	1.00
E-4		4	128.9	1.06	0.85		
E-6		6	126.5	1.04	0.83		
E-9		9	124.7	1.03	0.82		
F-2	0.3	2	134.7	1.11	0.89	0.92	0.90
F-4		4	118.7	0.98	0.78		
F-6		6	116.9	0.96	0.77		
F-9		9	115.1	0.95	0.76		
G-2	0.4	2	128.6	1.06	0.85	0.86	0.80
G-4		4	110.1	0.91	0.73		
G-6		6	108.4	0.89	0.71		
G-9		9	106.3	0.87	0.70		
H-2	0.5	2	115.7	0.95	0.76	0.80	0.70
H-4		4	99.8	0.82	0.66		
H-6		6	97.9	0.81	0.65		
H-9		9	96.2	0.79	0.63		

6. Conclusions

In order to investigate the behaviour of lying multi-stud connectors in cable-pylon anchorage zone, twenty-four push-out tests are carried out. The influence of number of studs and stud diameter are studied. The effect of concrete block width and tension force on shear strength is also parametrically analyzed. Strength and ductility obtained from the tests are evaluated, and a new expression of load-slip curve is proposed. The following conclusions can be drawn:

- Based on the test results, shear strength of the lying multi-stud connectors reduces compared with that of the lying single-stud connector, and the reduction increases with the increasing of stud number in the vertical direction. However, there is no obvious difference between the strength reductions of 22 mm and 25 mm studs. The maximum reductions of the specimens with 22 mm and 25 mm studs are 13.2% and 9.9%, respectively. EC 4 generally gives conservative predictions of the shear strength for lying multi-stud connectors, while AASHTO LRFD overestimates the shear strength.
- The average ultimate slips of the 25 mm lying studs is smaller than those of the 22 mm lying studs. Nevertheless, the characteristic ultimate slips of the lying studs with diameters of 22 mm and 25 mm are all larger than 6 mm and thus can be taken as ductile according to EC4. A new expression of load-slip curve is proposed for lying multi-stud connectors based on the test results and agrees better with the test results in comparison with those proposed by previous researchers.
- According to parametric analytical results, the concrete block width has a non-negligible effect on the shear strength of the lying multi-stud connectors. The smaller strength reduction of the test specimens with nine studs than the test specimens with six studs may be due to the difference of the concrete block widths. Therefore, the concrete block width should be chosen properly when designing push-out specimens.
- The influence of the number of studs on the strength reduction of lying multi-stud connectors decreases under combined shear and tension loads, yet the reduction due to multi-stud effect still cannot be ignored. Both the tri-linear and elliptical interaction equations are able to predict the interaction strength for lying multi-stud connectors reasonably.

References

AASHTO (2007), AASHTO LFRD Bridge Design Specifications; (4th Edition), American Associate of State Highway and Transportation Officials, Washington, D.C., USA.

ABAQUS (2010), Analysis User's Manual; (version 6.10), Hibbitt, Karlsson & Sorensen, USA.

Abbu, M.A., Ekmekyapar, T.A. and Özakça, M.A. (2014), "3D FE modeling considering shear connectors representation and number in CBGB", *Steel Compos*. *Struct*., *Int*. *J*., **17**(3), 237-252.

ACI 318-08 (2008), Building Code Requirements for Structure Concrete (ACI 318-08) and Commentary (ACI 318R-08); ACI, Farmington Hills, MI, USA.

Badie, S.S., Tadros, M.K., Kakish, H.F., Splittgerber, S.L. and Baishya, M.C. (2002), "Large shear studs for composite action in steel bridge girders", *J*. *Bridge Eng*. *ASCE*, **7**(3), 195-203.

Bode, H. and Roik, K. (1987), "Headed studs-embedded in concrete and loaded in tension", *Special Publication*, *ACI*, SP-103, 61-68.

Carreira, D.J. and Chu, K.H. (1985), "Stress-strain relationship for plain concrete in compression", *ACI J*. *Proceedings*, **82**(6), 797-804.

Cornelissen, H.A.W., Hordijk, D.A. and Reinhardt, H.W. (1986), "Experimental determination of crack softening characteristics of normal weight and lightweight concrete", *HERON*, **31**(2), 45-56.
Cook, R.A. and Klingner, R.E. (1989), "Behavior and design of ductile multiple anchor steel-to-concrete connections", Research Rep. No. 1126-3; Center for Transportation Research, University of Texas at Austin, Austin, TX, USA.
Eurocode 4 Part 1-1 (EC4-1-1) (2004), Eurocode 4: Design of composite steel and concrete structures − Part 1-1: General rules and rules for buildings; BS EN 1994-1-1 :2004, British Standards Institution, UK.
FIB-Fédération Internationale du Béton (2010), Model Code 2010 (first complete draft), bulletin 55, Volume 1, Lausanne, Switzerland.
Johnson, R.P. (2000), "Resistance of stud shear connectors to fatigue", *J. Constr. Steel Res.*, **56**(2), 101-116.
Hou, Z.M., Xia, H. and Zhang, Y.L. (2012), "Dynamic analysis and shear connector damage identification of steel-concrete composite beams", *Steel Compos. Struct.*, **13**(4), 327-341.
Kim, H.H. and Shim, C.S. (2009), "Experimental investigation of double composite twin-girder railway bridges", *J. Constr. Steel Res.*, **65**(6), 1355-1365.
Kuhlmann, U. and Kürschner, K. (2001), "Behavior of lying shear studs in reinforced concrete slabs", (Eligehausen R. Ed.), *Proceedings of International Symposium on Connections between Steel and Concrete*, Stuttgart, Germany, September, pp. 1076-1085.
Lam, D. and El-Lobody, E. (2005), "Behavior of headed stud shear connectors in composite beam", *J. Struct. Eng., ASCE*, **131**(1), 96-107.
Loh, H.Y., Uy, B. and Bradford, M.A. (2004), "The effects of partial shear connection in the hogging moment regions of composite beams Part II − Analytical study", *J. Constr. Steel Res.*, **60**(6), 921-962.
McMackin, P.J., Slutter, R.G. and Fisher, J.W. (1973), "Headed steel anchors under combined loading", *AISC Eng. J.*, **Second Quarter**, 43-52.
Mirza, O. and Uy, B. (2010), "Effects of the combination of axial and shear loading on the behaviour of headed stud steel anchors", *Eng. Struct.*, **32**(1), 93-105.
Nguyen, H.T. and Kim, S.E. (2009), "Finite element modeling of push-out tests for large stud shear connectors", *J. Constr. Steel Res.*, **65**(10), 1909-1920.
Oehlers, D.J. and Coughlan, C.G. (1986), "The shear stiffness of stud shear connections in composite beams", *J. Constr. Steel Res.*, **6**(4), 273-284.
Okada, J., Yoda, T. and Lebet, J.P. (2006), "A study of the group arrangements of stud connectors on shear strength behavior", *Struct. Eng. /Earthq. Eng.*, **23**(1), 75-89.
Ollgaard, J.G., Slutter, R.G. and Fisher, J.W. (1971), "Shear strength of stud connectors in lightweight and normal–weight concrete", *AISC Eng. J.*, **8**(2), 55-64.
Pallarés, L. and Hajjar, J.F. (2010), "Headed steel stud anchors in composite structures, Part II: Tension and interaction", *J. Constr. Steel Res.*, **66**(2), 213-228.
Qureshi, J., Lam, D. and Ye, J. (2011), "The influence of profiled sheeting thickness and shear connector's position on strength and ductility of headed shear connector", *Eng. Struct.*, **33**(5), 1643-1656.
Saari, W.K., Hajjar, J.F., Schultz, A.E. and Shield, C.K. (2004), "Behavior of shear studs in steel frames with reinforced concrete infill walls", *J. Constr. Steel Res.*, **60**(10), 1453-1480.
Shen, M.H. and Chung, K.F. (2011), "An investigation into shear resistance of headed shear studs in solid concrete slabs with local aggregates in Hong Kong", *Procedia Eng.*, **14**, 1098-1105.
Shim, C.S., Lee, P.G. and Yoon, T.Y. (2004), "Static behavior of large stud shear connectors", *Eng. Struct.*, **26**(12), 1853-1860.
Su, Q.T., Yang, G.T., Qin, F. and Wu, C. (2012), "Investigation on the horizontal mechanical behavior of steel-concrete composite cable-pylon anchorage", *J. Constr. Steel Res.*, **72**, 267-275.
Viest, I.M. (1956), "Investigation of stud shear connectors for composite concrete and steel *t*-beams", *ACI J. Proceedings*, **52**(4), 875-892.
Xu, C., Sugiura, K., Wu, C. and Su, Q.T. (2012), "Parametrical static analysis on group studs with typical push-out tests", *J. Constr. Steel Res.*, **72**, 84-96.
Xue, D.Y., Liu, Y.Q., Yu, Z. and He, J. (2012), "Static behavior of multi-stud shear connectors for steel-concrete composite bridge", *J. Constr. Steel Res.*, **74**, 1-7.

Zheng, S.J., Liu, Y.Q. and Xu, H.J. (2014), "Structural analysis of steel bracket-concrete walls in cable-tower composite anchorage", *Eng*. *Mech*., **31**(5), 197-202. [In Chinese]

DL